Article

Iron Chelation Properties of an Extracellular Siderophore Exochelin MN

Suraj Dhungana, Marvin J. Miller, Li Dong, Colin Ratledge, and Alvin L. Crumbliss

J. Am. Chem. Soc., **2003**, 125 (25), 7654-7663• DOI: 10.1021/ja029578u • Publication Date (Web): 30 May 2003

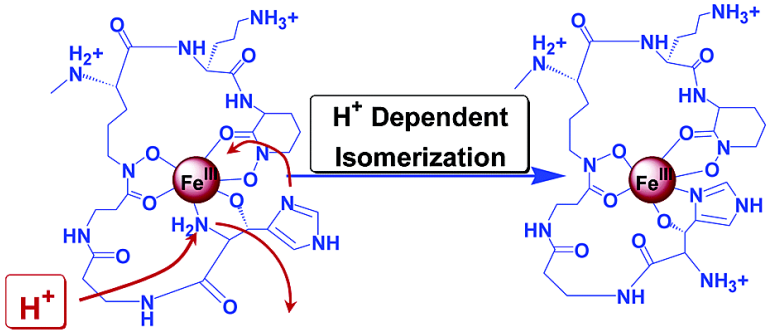

More About This Article

Additional resources and features associated with this article are available within the HTML version:

- Supporting Information
- Links to the 3 articles that cite this article, as of the time of this article download
- Access to high resolution figures
- Links to articles and content related to this article
- Copyright permission to reproduce figures and/or text from this article

View the Full Text HTML

J|A|C|S
ARTICLES
Published on Web 05/30/2003

Iron Chelation Properties of an Extracellular Siderophore Exochelin MN

Suraj Dhungana,[†] Marvin J. Miller,[‡] Li Dong,[‡] Colin Ratledge,[§] and Alvin L. Crumbliss*,[†]

Contribution from the Department of Chemistry, Duke University, Box 90346, Durham, North Carolina 27708-0346, Department of Chemistry and Biochemistry, University of Notre Dame, Notre Dame, Indiana 46556, and Department of Biological Sciences, University of Hull, Hull, HU6 7RX, U.K.

Received December 3, 2002; E-mail: alc@chem.duke.edu

Abstract: The coordination chemistry of an extracellular siderophore produced by *Mycobacterium neoaurum*, exochelin MN (ExoMN), is reported along with its pK_a values, Fe(III) and Fe(II) chelation constants, and aqueous solution speciation as determined by spectrophotometric and potentiometric titration techniques. Exochelin MN is of particular interest as it can efficiently transport iron into pathogenic *M. leprae*, which is responsible for leprosy, in addition to its own parent cells. The Fe(III) coordination properties of ExoMN are important with respect to understanding the Fe(III) acquisition and uptake mechanism in pathogenic *M. leprae*, as the siderophores from this organism are very difficult to isolate. Exochelin MN has two hydroxamic acid groups and an unusual *threo*-β-hydroxy-L-histidine available for Fe(III) chelation. The presence of *threo*-β-hydroxy-L-histidine gives rise to a unique mode of Fe(III) coordination. The pK_a values for the two hydroxamic acid moieties, the histidine imidazole ring and the alkylammonium groups on ExoMN, correspond well with the literature values for these moieties. Proton-dependent Fe(III)− and Fe(II)−ExoMN equilibrium constants were determined using a model involving sequential protonation of the Fe(III)− and Fe(II)−ExoMN complexes. These data were used to develop a model whereby deprotonation reactions on the surface of the complex in the second coordination shell result in first coordination shell isomerization. The overall formation constants were calculated: log $\beta_{110} = 39.12$ for Fe(III)−ExoMN and 16.7 for Fe(II)−ExoMN. The calculated pFe value of 31.1 is one of the highest among all siderophores and their synthetic analogues and indicates that ExoMN is thermodynamically capable of removing Fe(III) from transferrin. The $E_{1/2}$ for the Fe(III)ExoMN/Fe(II)ExoMN$^-$ couple was determined to be −595 mV from quasi-reversible cyclic voltammograms at pH = 10.8, and the pH-dependent $E_{1/2}$ profile was used to determine the Fe(II)−ExoMN protonation constants.

Introduction

Iron is an essential nutrient for virtually all living organisms. Under aqueous-aerobic conditions and neutral pH, iron is present mostly as insoluble Fe(III) hydroxide.[1] The total concentration of soluble iron ($Fe_{(aq)}^{3+} + Fe(OH)_{(aq)}^{2+} + Fe(OH)_{2(aq)}^{+}$) at pH = 7.4 and in the absence of chelating ligands is as low as 10^{-10} M,[2,3] a concentration that is 4 orders of magnitude lower than that required by microorganisms.[4] Microorganisms have evolved very specialized iron transport systems that are expressed under iron-deficient conditions. Siderophores, a class of low molecular weight and highly specific Fe(III) chelating agents, are synthesized by microorganisms to sequester iron from the environment. The siderophore−Fe(III) complex is taken up by cells in an energy-dependent process via specialized outer membrane receptor proteins. The ability of a microbe to express these specific membrane receptor proteins and efficiently assimilate Fe(III), under iron-deficient conditions, has proven to be an important virulence factor.[2,5−12]

Siderophores exhibit a high (log $\beta > 30$) and specific affinity for selective chelation of Fe(III) in the presence of other environmentally prevalent metal ions. These potent Fe(III)-specific chelators usually include either hydroxamate or cat-

[†] Duke University.
[‡] University of Notre Dame.
[§] University of Hull.

(1) Crichton, R. R. *Inorganic Biochemistry of Iron Metabolism: From Molecular Mechanism to Clinical Consequences*, 2nd ed.; Wiley: New York, 2001.
(2) Boukhalfa, H.; Crumbliss, A. L. *BioMetals* **2002**, *15*, 325−339.
(3) Chipperfield, J. R.; Ratledge, C. *BioMetals* **2000**, *13*, 165−168.
(4) Braun, V.; Killmann, H. *Trends Biol. Sci.* **1999**, *24*, 104−109.
(5) Albrecht-Gary, A.-M.; Crumbliss, A. L. In *Metal Ions in Biological Systems*; Sigel, A., Sigel, H., Eds.; Marcel Dekker: New York, 1998; Vol. 35, pp 239−328.
(6) Crumbliss, A. L. In *Handbook of Microbial Iron Chelates*; Winkelmann, G., Ed.; CRC Press: Boca Raton, FL, 1991; pp 177−233.
(7) Matzanke, B. F.; Müller-Matzanke, G.; Raymond, K. N. In *Iron Carriers and Iron Proteins*; Loehr, T. M., Ed.; VCH Publishers: New York, 1989; Vol. 5, pp 3−121.
(8) Neilands, J. B. *J. Biol. Chem.* **1995**, *270*, 26723−26726.
(9) Raymond, K. N.; Telford, J. R. In *NATO ASI Series C, Mathematical and Physical Sciences*; Kessissoglous, D. P., Ed.; Kluwer Academic Publishers: Dordrecht, The Netherlands, 1995; Vol. 459, pp 25−37.
(10) Winkelmann, G. *Handbook of Microbial Iron Chelates*; CRC Press: Boca Raton, FL, 1991.
(11) Ratledge, C.; Dover, L. G. *Annu. Rev. Microbiol.* **2000**, *54*, 881−941.
(12) Stintzi, A.; Raymond, K. N. In *Molecular and Cellular Iron Transport*; Templeton, D. M., Ed.; Marcel Dekker: New York, 2002; pp 273−320.

 10.1021/ja029578u CCC: $25.00

echolate functional groups for iron coordination.[5,6,9,12] However, in recent years, siderophores with new functional groups for iron coordination, including α-hydroxy carboxylic acid[5,12] and *β*-hydroxyhistidine,[13−15] have been identified and characterized. The high and specific Fe(III) chelating ability of siderophores easily overcomes the iron solubilization challenge, but in the process raises interesting questions regarding the Fe(III) release mechanism from these very stable siderophore−Fe(III) complexes. In the majority of cases, the iron release mechanism probably involves reduction of Fe(III) with removal and transfer of Fe(II) to various acceptor molecules within the bacterial cytoplasm;[2,11] less frequently occurring are mechanisms involving ligand exchange, hydrolysis of the siderophore ligand, and/or protonation of the iron−siderophore complex.[2,5]

Mycobacteria form a group that includes the pathogens *Mycobacterium leprae* and *Mycobacterium tuberculosis*, which are responsible for leprosy and tuberculosis, respectively. All mycobacteria, except *M. leprae* (see below), produce intracellular lipophilic siderophores, mycobactins,[16] and structurally related extracellular siderophores termed either exochelins, for the peptide-based, highly water-soluble molecules, or carboxymycobactins, in which the long alkyl chain of mycobactin is replaced with a short acyl chain or a terminally functionalized chain.[17] A large number of mycobactins have been isolated and characterized.[16] All mycobactins have a common core structure and are thought to hold Fe(III) within the cell envelope, allowing the iron (as Fe(II)) to be slowly released through the lipophilic cell membrane.[11,17] The extracellular exochelins/carboxymycobactins are responsible for sequestering Fe(III) from the aqueous-aerobic environment, including sources of iron within host tissues, and may transfer Fe(III) to the membrane-bound lipophilic mycobactins,[11,18,19] but in the case of the exochelins, they probably act as ligands for the transport of iron through the cell membrane itself. Excess iron, however, can be transferred from the exochelin to mycobactin to prevent sudden iron overloading of the cells.[17] All pathogenic mycobacteria that have been examined secrete carboxymycobactins as their sole extracellular siderophore. Saprophytic mycobacteria (including *Mycobacterium neoaurum* and *Mycobacterium smegmatis*), however, produce and utilize the peptide-based exochelins as their primary siderophore for Fe(III) acquisition.[13,17,20]

Exochelin MN (structure I), an extracellular siderophore produced by nonpathogenic *Mycobacterium neoaurum*, efficiently transports iron into the pathogenic *M. leprae* in addition to its own cells.[13,22] Exochelins from other species of myco-

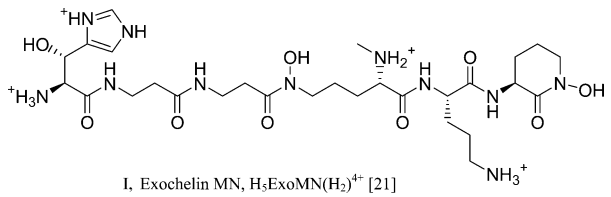

I, Exochelin MN, $H_5ExoMN(H_2)^{4+}$ [21]

bacteria cannot mediate iron transport in *M. leprae*, unlike exochelin MN. This strongly suggests structural similarities between the siderophores of *M. neoaurum* and *M. leprae* as well as similarities in the specific iron uptake mechanism of these two species. *M. leprae* cannot be grown in laboratory culture, but can only be obtained from either armadillos or infected foot-pads of mice.[13] Thus, its exochelin is hard to recover and difficult to identify. Following the sequencing of the genome of *M. leprae*,[23] an analysis of its genes has failed to identify genes for the biosynthesis of mycobactin or carboxymycobactin.[24] There are, however, genes coding for polyketide synthesases of unknown function that could be involved in the biosynthesis of an exochelin, but these are not related to the genes for exochelin MS biosynthesis in *M. smegmatis*. Only by appropriate gene sequencing in *M. neoaurum*, followed by searching the *M. leprae* genome, will it be possible to confirm if *M. leprae* does indeed have the capacity to synthesize an exochelin related to exochelin MN. This challenge makes the structural information of exochelin MN and its Fe(III) chelation properties important with regard to understanding the iron acquisition mechanism in pathogenic *M. leprae*. *M. neoaurum* is nonpathogenic, and, although it has seldom been encountered in human disease, very recently a few cases of infection related to *M. neoaurum* have been reported.[25−27] Such a finding adds extra significance to obtaining a better understanding of the iron uptake mechanism in these organisms.

The structure of exochelin MN (structure I) includes a hexapeptide backbone characterized by two hydroxamic acid groups and an unusual amino acid moiety, *threo*-*β*-hydroxy-L-histidine.[13] This unusual residue has been found in only one other siderophore, pseudobactin PF224.[15] Previous studies have shown that exochelin MN coordinates Ga(III) octahedrally via two *cis*-hydroxamate groups and the hydroxyl oxygen and the imidazole nitrogen of the *threo*-*β*-hydroxy-L-histidine residue at pH = 6.[13] Such a mode of coordination is interesting and has not previously been characterized. A complete solution and thermodynamic characterization of the Fe(III)−exochelin MN complex as a function of pH will provide the details of this unique coordination mode involving *β*-hydroxyhistidine and give information relevant to the iron acquisition and uptake mech-

(13) Sharman, G. J.; Williams, D. H.; Ewing, D. F.; Ratledge, C. *Chem. Biol.* **1995**, *2*, 553−561.
(14) Dong, L.; Miller, M. J. *J. Org. Chem.* **2002**, *67*, 4759−4770.
(15) Hancock, D. K.; Coxon, B.; Wang, S. Y.; White, E. V.; Reeder, D. J.; Bellama, J. M. *J. Chem. Soc., Chem. Commun.* **1993**, 468−469.
(16) Snow, G. A. *Bacteriol. Rev.* **1970**, *34*, 99−125.
(17) Ratledge, C. In *Mycobacteria: Molecular Biology and Virulence*; Ratledge, C., Dale, J., Eds.; Blackwell Science Publishers Ltd.: Oxford, U.K., 1999; pp 260−286.
(18) Wheeler, P. R.; Ratledge, C. In *Tuberculosis Pathogenesis, Protection, and Control*; Bloom, B. R., Ed.; American Society of Microbiology: Washington, DC, 1994; p 353.
(19) Ratledge, C. In *Iron Transport in Microbes, Plants and Animals*; Winkelmann, G., van der Helm, D., Neilands, J. B., Eds.; VCH Publishers: Weinheim, 1987; pp 207−221.
(20) Sharman, G. J.; Williams, D. H.; Ewing, D. F.; Ratledge, C. *Biochem. J.* **1995**, *305*, 187−196.
(21) Exochelin MN in its fully protonated form is represented by $H_5ExoMN(H_2)^{4+}$, where the "H_5" component represents the five ionizable protons associated with donor groups directly bound to Fe(III) in the first coordination sphere (two hydroxamate, one amine, one hydroxyl, and one imidazole) and the "H_2" component represents the two ionizable protons associated with a primary and secondary amine not coordinated to Fe(III) in the second coordination sphere. See Schemes 1 and 2 for structural elucidation.
(22) Hall, R. M.; Ratledge, C. *J. Gen. Microbiol.* **1987**, *133*, 193−199.
(23) Cole, S. T.; Eigimeier, K.; Parkhill, J.; James, K. D.; Thomson, N. R.; Wheeler, P. R.; Honore, N.; Garnier, T.; Churcher, C.; Harris, D.; Mungall, K.; Basham, D.; Brown, D.; Chillingworth, T.; Connor, R.; Davies, R. M.; Devlin, K.; Duthoy, S.; Feltwell, T.; Fraser, A.; Hamlim, N.; Holroyd, S.; Hornsby, T.; Jagels, K.; Lacroix, C.; Maclean, J.; Moule, S.; Murphy, L.; Oliver, K.; Quail, M. A.; Rajandream, M. A.; Rutherford, K. M.; Rutter, S.; Seeger, K.; Simon, S.; Simmonds, M.; Skelton, J.; Squares, R.; Stevens, K.; Taylor, K.; Whitehead, S.; Woodward, J. R.; Barrell, B. G. *Nature (London, United Kingdom)* **2001**, *409*, 1007−1011.
(24) Wheeler, P. R. *World J. Microbiol. Biotechnol.* **2003**, *19*, 1−16.
(25) Davidson, M. B.; McCormack, J. G.; Blacklock, Z. M.; Dawson, D. J.; Tilse, M. H.; Crimmins, F. B. *J. Clin. Microbiol.* **1988**, *26*, 762−764.
(26) George, S. L.; Schlesinger, L. S. *Clin. Infect. Dis.* **1999**, *28*, 682−683.
(27) Holland, D. J.; Chen, S. C.; Chew, W. W.; Gilbert, G. L. *Clin. Infect. Dis.* **1994**, *18*, 1002−1003.

anism in both *M. neoaurum* and *M. leprae*. A better understanding of the specific activity of exochelin MN in *M. leprae* could be used to design drugs targeting the exochelin MN iron transport pathways to combat against infection caused by this pathogen. This article describes the complete aqueous solution characterization of the Fe(III) and Fe(II) chelating ability of exochelin MN over a wide pH range.

Experimental Section

Materials. All solutions were prepared in deionized water. All pH measurements were made using a Corning 250 pH/ion meter equipped with an Orion ROSS pH electrode filled with 3 M NaCl solution.

The pH of all solutions was adjusted with NaOH or $HClO_4$, accordingly. A stock solution of 2 M $NaClO_4$ was prepared from solid sodium perchlorate hydrate (Aldrich 99+%) and standardized by passing through a Dowex 50 W-X8 strong acid cation-exchange column in H^+ form. The acid displaced from the column was titrated with standard NaOH solution to the phenolphthalein end point. A 2 M $HClO_4$ stock solution was prepared from concentrated perchloric acid (Fisher 70%) and standardized by titration with standard NaOH solution to the phenolphthalein end point. A Fe(III) perchlorate stock solution (0.1 M) was prepared from recrystallized Fe(III) perchlorate (Aldrich), standardized spectrophotometrically in strong acid[28] and titrimetrically by reduction with Sn(II), and titrated with the primary standard potassium dichromate.[29] Carbonate-free NaOH was prepared by diluting 1 M NaOH with deionized water purged with Ar for 45 min and standardized by titration with standard 0.2 M HCl to the phenolphthalein end point. A glass bulb electrode (Corning high performance) was used for the measurement of pH. The glass electrode was calibrated to read pH according to the classical method.[30]

The exochelin MN was isolated and purified following the procedure published earlier.[13] The Fe(III)-exochelin MN was reduced with a few crystals of sodium dithionate under a stream of nitrogen. The colorless solution was passed through a gel-permeation column (Sephadex G-10; 55 cm × 3 cm) and was eluted with deoxygenated DI water. Red-colored exochelin MN was collected and concentrated, and the process was repeated. The second elution yielded a colorless solution which was checked by spotting with $FeCl_3$ solution, and its conductivity was simultaneously monitored to exclude salts. The eluant was concentrated and stored under anaerobic conditions.

Methods. Potentiometric Measurements. Samples (10 mL) were placed in a double-walled titration cell maintained at 25.00 ± 0.05 °C by a circulating constant-temperature bath. Solutions were adjusted to $I = 0.1$ by the addition of 2 M $NaClO_4$, and all solutions were purged with Ar prior to titration. A Titronic 96 standard buret was used for the titration; data were analyzed by the program SUPERQUAD.[31] The uncertainties in pK_a values were calculated from the standard deviation.

Spectrophotometric Measurements. UV−visible spectra were recorded using a Cary 100 spectrophotometer. All solutions were adjusted to $I = 0.1$ by the addition of 2 M $NaClO_4$. UV−visible spectra of the iron complexes as a function of pH were obtained from a single stock solution containing a 1:1 ratio of exochelin MN:Fe^{3+}, where each species is 3.3×10^{-4} M. The stock solution was divided into three different aliquots, and each aliquot was used separately for a spectrophotometric titration. Titrations were carried out in both directions, from low pH to high pH and from high pH to low pH, using different aliquots of iron complexes. After each adjustment of pH, the solution was allowed to equilibrate for 20−30 min, and its visible spectrum was recorded. Corrections were made for dilution due to the addition of acid and base; data were analyzed using the SPECFIT/32 software.[32] The uncertainties in log β and the protonation constants were calculated from the standard deviation.

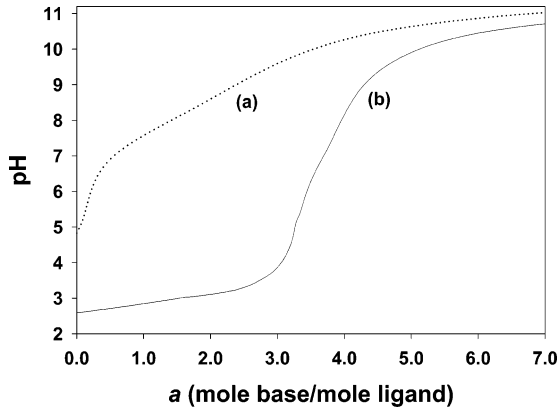

Figure 1. Potentiometric titration curves: (a) 1.4×10^{-3} M exochelin MN; (b) exochelin MN and Fe^{3+}, 1:1, 5.4×10^{-4} M. Conditions: $T = 298$ K and $I = 0.10$ M $NaClO_4$.

In another series, spectrophotometric experiments involving competition with EDTA were carried out at a fixed pH of 10.8. Samples (5 mL) were allowed to equilibrate with various EDTA concentrations for a week at 25 °C. Typical solutions were 3.3×10^{-4} M in Fe(III) and the exochelin MN ligand, with up to a 10-fold excess of EDTA (Aldrich). The protonation and Fe(III) formation constants for EDTA were taken from the critical compilation of Martell and Smith.[33]

Electrochemistry. The electrochemical behavior of the Fe(III)−exochelin MN complex was studied in aqueous solution under an Ar atmosphere at room temperature with 0.1 M $NaClO_4$ as supporting electrolyte. Voltammograms were obtained using an EG&G Princeton Applied Research potentiostat, model 263, at a scan rate of 20 mV/s, with a HDME working electrode, Ag/AgCl (KCl saturated) reference electrode, and platinum wire auxiliary electrode, and recorded using PowerCV cyclic voltammetry software. Typical solutions were 5×10^{-3} M in Fe(III) and 3.5×10^{-2} M in ligand. The pH of the solution was adjusted using 1 M NaOH and 2 M $HClO_4$. Potentials referenced to Ag/AgCl (KCl saturated) were converted into NHE by adding 197 mV.

Results

Ligand Deprotonation Constants. Exochelin MN (ExoMN) (structure I) is very soluble in water and when dissolved in 0.1 M $NaClO_4$ gives a solution of pH 5.8. ExoMN has seven different deprotonation sites: two hydroxamic acid groups, two primary amines, a secondary amine, an imidazole, and a hydroxyl group of β-hydroxyhistidine. Six of the seven deprotonation constants were determined by potentiometric titration. The acidity of the hydroxyl group could not be determined, because it is beyond the pH range of our experiments. The potentiometric equilibrium curves for free ExoMN and its Fe(III)-complex are shown in Figure 1. The ligand deprotonation constants, K_{an} ($n = 1, 2, ...7$), are defined by eqs 1 and 2 and are listed in Table 1 as pK_{an} ($-\log(K_{an})$).

$$H_{8-n}\text{ExoMN}^{+5-n} \overset{K_{an}}{\rightleftharpoons} H_{7-n}\text{ExoMN}^{+4-n} + H^+ \qquad (1)$$

$$K_{an} = \frac{[H_{7-n}\text{ExoMN}^{+4-n}][H^+]}{[H_{8-n}\text{ExoMN}^{+5-n}]} \qquad (2)$$

The six acid dissociation constants determined for ExoMN represent three different acidic groups. The first deprotonation

(28) Bastian, R.; Weberling, R.; Palilla, F. *Anal. Chem.* **1956**, *28*, 459−462.
(29) Vogel, A. I. *Quantitative Inorganic Analysis Including Elementary Instrumental Analysis*, 3rd ed.; Longmans, Green and Co., Ltd.: London, 1968.
(30) Martell, A. E.; Motekaitis, R. J. *Determination and Use of Stability Constants*, 2nd ed.; VCH Publishers: New York, 1992.
(31) Gans, P.; Sabatini, A.; Vacca, A. *J. Chem. Soc., Dalton Trans.* **1985**, 1195−1200.

Table 1. Ligand pK_a Values for Exochelin MN[a]

n	pK_{an}
1	7.09 ± 0.06
2	8.01 ± 0.06
3	9.07 ± 0.05
4	10.03 ± 0.05
5	10.73 ± 0.03
6	10.79 ± 0.04
7	13.5[b]

[a] See equilibrium eqs 1 and 2. Conditions: $T = 298$ K and $I = 0.10$ M $NaClO_4$. The uncertainties in the protonation constants were calculated from the standard deviation. [b] Estimated for the hydroxyl group based on the primary alcohol with α inductive groups.

constant, pK_{a1} = 7.09, is assigned to the deprotonation of the imidazole nitrogen of the histidine moiety. This deprotonation constant is in very good agreement with that seen for imidazole (pK_a = 7.03) and other substituted imidazoles (pK_a = 6.3−7.6).[33] The second and the third acid dissociation constants are assigned to the dissociation of the two hydroxamic acids. The pK_{a2} value of 8.01 is assigned to the six-membered cyclic hydroxamic acid group, and the pK_{a3} value of 9.07 is assigned to the linear backbone hydroxamic acid. These assignments are made on the basis of their values falling within the normal range (pK_a = 8−10) for hydroxamic acids[34−36] and the fact that the cyclic hydroxamic acid has an amide moiety α to the carbonyl group and the linear hydroxamic acid has an amide moiety β to the carbonyl group. The inductive effect of an α-amino substitution is well established and is known to lower the pK_a significantly (alanine hydroxamic acid has a pK_a of 7.26, whereas β-alanine hydroxamic acid has a higher pK_a of 8.37).[33] The fourth, fifth, and sixth proton dissociation constants correspond to the deprotonation of the three alkylammonium groups. The pK_{a4} value of 10.03 is assigned to the secondary alkylammonium moiety. The almost identical pK_{a5} and pK_{a6} values of 10.73 and 10.79 are assigned to the two primary alkylammonium moieties in an arbitrary fashion. The pK_a values of all three alkylammonium groups are in good agreement with the pK_a values of similar alkylammonium moieties.[33] The deprotonation constant corresponding to the hydroxyl group of the β-hydroxyhistidine could not be directly determined and was estimated to be 13.5.

Fe(III)-Complex Formation and Protonation Constants. General Considerations. The potentiometric titration curve for ExoMN in the presence of an equivalent concentration of Fe(III) (Figure 1) shows that a total of five protons, $a = 5$, are released upon Fe(III) binding. The first three protons, $a = 3$, are released relatively easily upon the addition of Fe(III) and give rise to a buffer region in the lower part of the titration curve. The titration curve exhibits a large jump beyond $a = 3$ which lasts until $a = 5$. A clear inflection point is seen at $a = 4$ in the pH range 7.9−8.1. The steep rise of the titration curve, representing the tight binding of Fe(III), clearly indicates a release of five protons upon Fe(III) binding. Beyond $a = 5$, the titration curve displays another buffer region involving two protons.

(32) Binstead, R. A.; Jung, B.; Zuberbühler, A. D. *SPECFIT/32 Global Analysis System*, 3.0 ed.; Spectrum Software Associates: Marlborough, MA, 2000.
(33) Martell, A. E.; Smith, R. M. *Critical Stability Constants*; Plenum Press: New York, 2001; Vol. 1.
(34) Monzyk, B.; Crumbliss, A. L. *J. Org. Chem.* **1980**, *45*, 4670−4675.
(35) Brink, C. P.; Crumbliss, A. L. *J. Org. Chem.* **1982**, *47*, 1171−1176.
(36) Brink, C. P.; Fish, L. L.; Crumbliss, A. L. *J. Org. Chem.* **1985**, *50*, 2277−2281.

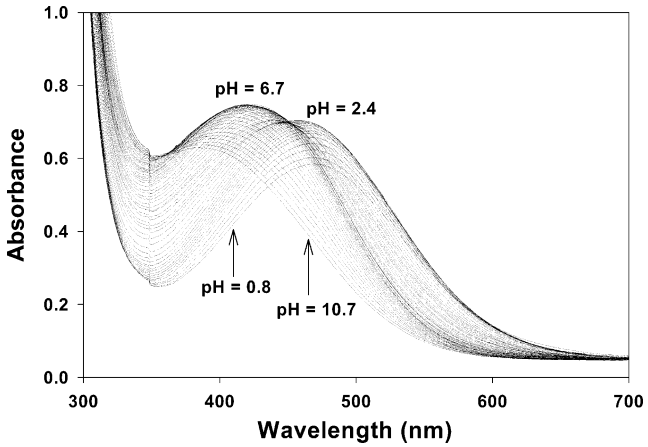

Figure 2. Spectrophotometric titration: UV−visible spectra of Fe(III)−exochelin MN as a function of pH from pH 0.77 to 10.8. Conditions: exochelin MN and Fe^{3+}, 1:1, 3.3×10^{-4} M. $T = 298$ K and $I = 0.10$ M $NaClO_4$.

The spectrophotometric titration of ExoMN in the presence of Fe(III) was carried out separately in both directions, from low pH to high pH and from high pH to low pH, with identical results. The ligand-to-metal charge transfer (LMCT) bands are completely reversible in both sets of experiments and indicate no significant ligand hydrolysis at both acidic and basic pH. A spectral profile for the titration going from high pH to low pH is shown in Figure 2. Above pH = 10.8, there was no significant change in the LMCT bands, $\lambda_{max} = 385$ nm ($\epsilon = 1910$ M^{-1} cm^{-1}), indicating the presence of only one Fe(III)−ExoMN species. Three additional absorption maxima corresponding to LMCT bands are observed as the pH of the Fe(III)−ExoMN complex was lowered from pH = 10.8 to 0.8: $\lambda_{max} = 423$ nm ($\epsilon = 2270$ M^{-1} cm^{-1}) at pH = 6.7, $\lambda_{max} = 460$ nm ($\epsilon = 2130$ M^{-1} cm^{-1}) at pH = 2.4, and $\lambda_{max} = 470$ nm ($\epsilon = 1770$ M^{-1} cm^{-1}) at pH = 0.8.

Fe(III)−Exochelin MN Complex Equilibria. The potentiometric titration curve for ExoMN in the presence of Fe(III) establishes the number of protons involved in the Fe(III)−ExoMN equilibria and the pH range of their involvement. The three proton buffer region, which covers the pH range 2.6−3.9, indicates that three protons are rather easily displaced from ExoMN by Fe(III) as the Fe(III)−ExoMN complexation starts. The buffer region also suggests that the first three pK_a's associated with the liberated protons from Fe(III)−ExoMN lie well below pH = 3.9. The steep jump of the titration curve starts just after $a = 3$ and extends until $a = 5$. This steepness underlines the tight binding of Fe(III) by ExoMN, and in the process two more protons are liberated from the ligand. The presence of an inflection point at $a = 4$ suggests that these two protons are released in two distinct steps during the complexation process. The pH values corresponding to $a = 3.5$ and $a = 4.5$ (half equivalence points) represent the fourth and fifth pK_a's of the Fe(III)−ExoMN complex and are calculated to be 6.98 and 9.61, respectively, using the program SUPERQUAD.[31] The potentiometric titration data refinement further allowed for the calculation of two more pK_a's corresponding to the liberation of the sixth ($a = 6$) and the seventh ($a = 7$) protons. These pK_a's were found to be 10.24 and 10.7, respectively, and were assigned as the proton dissociations of the secondary and primary alkylammonium moieties present in the second coordination shell of Fe(III) (backbone of the ExoMN molecule).

This assignment is consistent with primary alkylammonium moieties having a higher pK_a than a secondary alkylammonium. These pK_a values are in very good agreement with those determined for the Fe(III)−free ExoMN. The titration curve between $a = 5$ and $a = 7$ is not steep, which is consistent with proton dissociation taking place in the second coordination shell of Fe(III).

The spectrophotometric titration of the Fe(III)−ExoMN complex allows one to study the proton-dependent Fe(III)−ExoMN equilibria by observing the changes in the intense LMCT band of the metal complex (Figure 2). As discussed earlier, the pH-dependent spectral profile clearly indicates the presence of four different forms of Fe(III)−ExoMN complexes. The $\lambda_{max} = 470$ nm ($\epsilon = 1770$ M^{-1} cm^{-1}) observed at pH = 0.87 is characteristic of a bishydroxamate complex of Fe(III)[6] and suggests that the Fe(III) complexation by ExoMN at low pH begins with the coordination of Fe(III) by the two hydroxamate groups. At a slightly higher pH of 2.4, the λ_{max} shifts to 460 nm ($\epsilon = 2130$ M^{-1} cm^{-1}). This small yet distinct shift in the LMCT band is assigned to pentacoordinate Fe(III) formed by the addition of imidazole nitrogen to the first coordination shell with simultaneous liberation of a proton. The observed small shift in λ_{max} is consistent with coordination by the imidazole nitrogen, as it acts as a soft monodentate ligand. The Fe(III)−ExoMN complex has a distinct absorption maximum, $\lambda_{max} = 423$ nm ($\epsilon = 2270$ M^{-1} cm^{-1}), at pH = 6.7. This λ_{max} indicates the presence of a third form of Fe(III)−ExoMN in solution. This LMCT band is assigned to the complete coordination of Fe(III) by exochelin MN, where the sixth coordination site on the Fe(III) is occupied by the oxygen atom of the hydroxyl group. This structural characterization of the Fe(III)−ExoMN complex, involving the coordination of Fe(III) by two hydroxamate groups and a β-hydroxy histidine, is consistent with that seen for the Ga(III)−ExoMN complex at pH = 6 using NMR methods.[13] The fourth and final absorption band seen at pH 10.7 and above with $\lambda_{max} = 385$ nm ($\epsilon = 1910$ M^{-1} cm^{-1}) is not a result of the hydrolysis of the Fe(III)−ExoMN complex, as the reaction retains its full reversibility. At this point, ExoMN has already saturated the six coordination sites on Fe(III). Therefore, this observed unusual LMCT band is a result of a shift in the Fe(III) coordination mode. At such a high pH, the primary alkylammonium moiety adjacent to the hydroxyl group on ExoMN releases a proton and coordinates to Fe(III) by displacing the softer imidazole nitrogen atom. The spectrophotometric data were analyzed using the program SPECFIT,[32] and three different pK_a values of 0.90, 2.39, and 6.58 were extracted. These pK_a values, associated with the protons released from ExoMN upon the binding of Fe(III), were easy to calculate from the spectrophotometric titration as compared to potentiometric titration, as the Fe(III)−ExoMN complexes display a distinct spectral profile in the low pH range.

When taken together, the potentiometric and spectrophotometric data give a clear picture of the Fe(III) complexation process by exochelin MN, along with the pK_a values of the Fe(III)−ExoMN complex. Spectrophotometric data show that the Fe(III) coordination by ExoMN initiates at a very low pH. All of the Fe(III)−ExoMN complex pK_a values are listed in Table 2. At pH = 0.87, as discussed earlier, two hydroxamate groups are already coordinated to Fe(III). The pK_a value of 0.90 calculated from the spectrophotometric titration is assigned to the release of the second proton from ExoMN upon Fe(III) binding by the second hydroxamate group. Equations 3 and 4 summarize the process of Fe(III) chelation and simultaneous release of protons

Table 2. pK_a Values and Protonation Constants for Fe−Exochelin MN Complexes[a]

	Fe(III)[b]	Fe(II)
$pK_2 = \log K_{FeH_4ExoMN(H_2)}$	0.90 ± 0.20[c]	
$pK_3 = \log K_{FeH_3ExoMN(H_2)}$	2.39 ± 0.10[c]	
$pK_4 = \log K_{FeH_2ExoMN(H_2)}$	6.58 ± 0.05[c]	8.9 ± 0.1[d,e]
	6.98 ± 0.14[f]	
$pK_5 = \log K_{FeHExoMN(H_2)}$	9.61 ± 0.05[f]	10.3 ± 0.2[d,g]
$pK_6 = \log K_{FeExoMN(H_2)}$	10.24 ± 0.05[f]	
$pK_7 = \log K_{FeExoMN(H)}$	10.7 ± 0.1[f]	

[a] Conditions: $T = 298$ K and $I = 0.10$ M $NaClO_4$. The uncertainties in the protonation constants were calculated from the standard deviation. [b] See Scheme 2 for equilibria corresponding to pK_n ($n = 2-7$) and $K_{Fe(III)H_xExoMN(H_y)}$. [c] Spectrophotometric titration. [d] Calculated from pH-dependent $E_{1/2}$. [e] See eqs 19 and 20 for equilibrium expressions. [f] Potentiometric titration. [g] See eqs 17 and 18 for equilibrium expressions.

$$Fe(III)H_4ExoMN(H_2)(H_2O)_4^{6+} \overset{K_2}{\rightleftharpoons} Fe(III)H_3ExoMN(H_2)(H_2O)_2^{5+} + H^+ \quad (3)$$

$$K_2 = \frac{[Fe(III)H_3ExoMN(H_2)(H_2O)_2^{5+}][H^+]}{[Fe(III)H_4ExoMN(H_2)(H_2O)_4^{6+}]} \quad (4)$$

where $Fe(III)H_4ExoMN(H_2)(H_2O)_4^{6+}$ is the complex with one hydroxamate group coordinated to Fe(III), and $Fe(III)H_3ExoMN(H_2)(H_2O)_2^{5+}$ is the complex with two hydroxamate groups coordinated to Fe(III).[21]

Similarly, the Fe(III)-ExoMN complex pK_a values of 2.39 (spectrophotometric), 6.58 (spectophotometric) and 6.98 (potentiometric), and 9.61 (potentiometric) represent the release of the third (pK_3), fourth (pK_4), and fifth (pK_5) protons, respectively, with simultaneous coordination of Fe(III) by ExoMN, in distinct steps. The stepwise equilibria are represented by eqs 5 and 6; the water molecules involved in the equilibria are omitted for simplicity and $pK_n = -\log K_n$.

$$\{Fe(III)-ExoMNH_{8-n}\}^{+8-n} \overset{K_n}{\rightleftharpoons} \{Fe(III)-ExoMNH_{7-n}\}^{+7-n} + H^+ \quad (5)$$

$$K_n = \frac{[\{Fe(III)-ExoMNH_{7-n}\}^{+7-n}][H^+]}{[\{Fe(III)-ExoMNH_{8-n}\}^{+8-n}]} \quad (6)$$

The pK_3 value of 2.39 is assigned to the proton released upon Fe(III) coordination by the imidazole nitrogen. The pK_4 value obtained from the potentiometric titration, 6.98, is in very good agreement with that obtained from the spectrophotometric titration, 6.58, and is assigned to the proton liberated upon Fe(III) coordination by the hydroxyl group of β-hydroxyhistidine. The pK_5 value obtained for the potentiometric titration, 9.61, is assigned to the proton liberated upon Fe(III) coordination by the primary amine adjacent to the hydroxyl group of β-hydroxyhistidine. This coordination involves the replacement of imidazole nitrogen by the primary amine nitrogen in the first coordination shell of iron. Such a proton-driven ligand donor atom exchange results in a coordination isomerization of the Fe(III)−ExoMN complex which will be discussed later. The

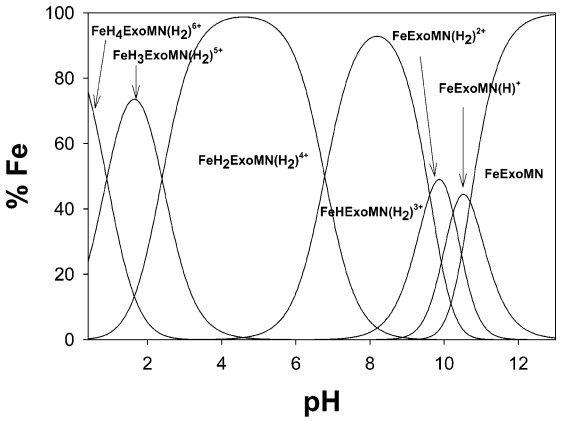

Figure 3. Calculated species distribution for Fe(III)-complexes of exochelin MN. Metal containing species are normalized to the total concentration of iron. Coordinated water molecules are omitted for clarity. Conditions: [exochelin MN]:[Fe^{3+}] = 1:1. T = 298 K and I = 0.10 M $NaClO_4$.

Scheme 1

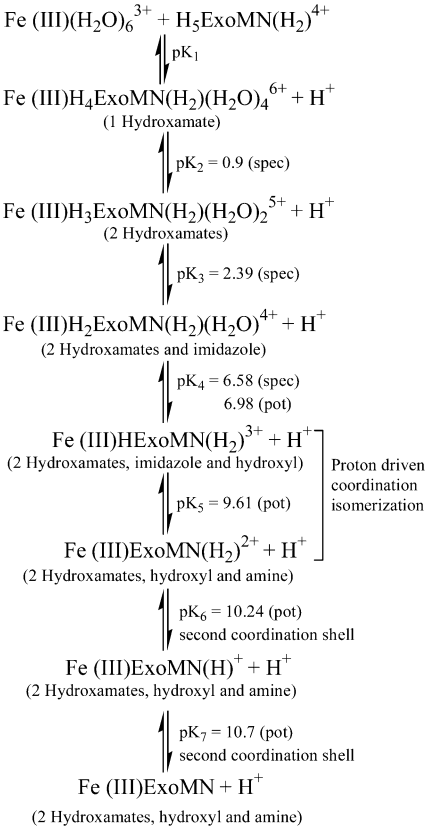

pK_6 and pK_7 values were assigned as proton dissociations from the secondary and primary alkylammonium moieties present in the second coordination shell of Fe(III).

The potentiometric and spectrophotometric results are summarized in Scheme 1 in the context of Fe(III)−ExoMN complex formation.[21]

Overall Complex Stability and Species Distribution. The pK_a values determined for the Fe(III)−ExoMN complex (Table 2) were used to generate a species distribution plot (Figure 3). The speciation diagram for the Fe(III)−ExoMN system clearly shows three species as the predominant Fe(III)−ExoMn complexes in different pH regimes: Fe(III)ExoMN above pH = 10.7, Fe(III)HExo$(H_2)^{3+}$ at pH = 8, and Fe(III)H_2Exo$(H_2)^{4+}$ at pH = 5.[21]

Table 3. Fe−Siderophore Complex Thermodynamic Parameters

siderophore	log β_{110}[a] Fe(III)	log β_{110}[a] Fe(II)	pFe[b]	$E_{1/2}$ vs NHE (mV)	ref
exochelin MN	39.12 ± 0.17[c]	16.7[c,d]	31.1[c]	−595[c]	this work
desferrichrome	29.07	9.9	25.2	−400	38,39,50
desferricrocin	30.4	11.6	26.5	−412	38
desferrioxamine B	30.60	10.3	26.6	−468	37,51−53
pyoverdin PaA	30.8	9.8	27	−510	41
enterobactin	49	23.9	35.5	−750	40,54,55

[a] Defined as β_{110} = [FeL]/[Fe][L] for Fe + L ⇌ FeL (charges omitted for clarity). [b] −log[Fe^{3+}] at $[Fe(III)]_{tot} = 10^{-6}$ M, $[ligand]_{tot} = 10^{-5}$ M, and pH = 7.4. [c] Conditions: T = 298 K and I = 0.10 M $NaClO_4$. The uncertainty in the log β value was calculated from the standard deviation. [d] Calculated from eq 15 using E_{aquo} = +732 mV, consistent with our previous work.[53]

The overall stability constant, log β_{110}^{III} (defined by eqs 7 and 8), for Fe(III)−ExoMN was calculated using the software SPECFIT[32] and data from the spectrophotometric titration (Table 3). Ligand pK_a values for the amine protons that do not participate in Fe(III) coordination were not included in the calculation of the overall stability constant. The Fe(III)−ExoMN equilibrium exhibits one of the highest log β_{110}^{III} observed for natural siderophores.[5,37−41]

$$Fe_{(aq)}^{3+} + ExoMN^{3-} \rightleftharpoons FeExoMN \quad (7)$$

$$\beta_{110}^{III} = \frac{[FeExoMN]}{[Fe_{(aq)}^{3+}][ExoMN^{3-}]} \quad (8)$$

The overall stability of the Fe(III)-complexes of ExoMN (log β_{110}^{III}) was also determined by spectrophotometric competition experiments with EDTA at pH 10.8. The competition equilibrium is described by eqs 9 and 10.

$$Fe(III)-ExoMN + EDTA \overset{K}{\rightleftharpoons} Fe(III)-EDTA + ExoMN \quad (9)$$

$$K = \frac{[Fe(III)-EDTA][ExoMN]}{[Fe(III)-ExoMN][EDTA]} = \frac{\beta^{FeEDTA}}{\beta^{Fe(III)ExoMN}} \quad (10)$$

The molecular charges, degree of EDTA and ExoMN protonation, and water molecules involved in the equilibrium are omitted for clarity. Fe(III)−EDTA represents all protonated and hydrolyzed forms of Fe(III)−EDTA present at pH 10.8. β^{FeEDTA} and $\beta^{FeExoMN}$ represent the effective binding of EDTA and ExoMN at the experimental pH (10.8). The equilibrium concentrations of Fe(III)−ExoMN at various competing EDTA concentrations were calculated from the absorbance at 385 nm, where Fe(III)−ExoMN is the only light absorbing species. The concentrations of other species in eq 10 were calculated from mass balance equations using the experimental pH values

$$[Fe]_{Tot} = \alpha_{Fe(III)ExoMN}[Fe(III)-ExoMN] + \alpha_{Fe(III)EDTA}[Fe(III)-EDTA] \quad (11)$$

$$[ExoMN]_{Tot} = \alpha_{Fe(III)ExoMN}[Fe(III)-ExoMN] + \alpha_{ExoMN}[ExoMN] \quad (12)$$

$$[EDTA]_{Tot} = \alpha_{Fe(III)EDTA}[Fe(III)-EDTA] + \alpha_{EDTA}[EDTA] \quad (13)$$

where α is the usual Ringbom's coefficient.[42] The stability constant, log β_{110}^{III}, for Fe(III)−ExoMN was calculated using

the relationship defined by eq 10 and found to be 38.8, in excellent agreement with the value determined from the spectrophotometric titration (Table 3).

To compare the Fe(III) chelating properties of ExoMN with other Fe(III) chelators at physiological conditions, the pFe value was calculated ($-\log[Fe^{3+}]$ at pH = 7.4 with a total ligand concentration ($[L]_{tot}$) of 10^{-5} M and total Fe(III) concentration of 10^{-6} M).[43] The concentration of free Fe^{3+} ion in solution can be expressed by eq 14

$$[Fe^{3+}] = \frac{[Fe(III)-ExoMN]}{\beta_{110}^{III}[ExoMN]} = \frac{[Fe(III)-ExoMN]_{tot}\alpha_{ExoMN}}{\beta_{110}^{III}[ExoMN]_{tot}\alpha_{Fe(III)ExoMN}} = \frac{[Fe(III)-ExoMN]_{tot}\alpha_{ExoMN}}{\beta_{110}^{III}[(ExoMN)_o - (Fe(III)-ExoMN)_{tot}]\alpha_{Fe(III)ExoMN}} = \frac{\alpha_{ExoMN}}{9\alpha_{Fe(III)ExoMN}\beta_{110}^{III}} \quad (14)$$

where β_{110}^{III} represents the overall stability constant for the 1:1 Fe(III)-complex, $[(ExoMN)_o]$ is the initial concentration of ExoMN, and α_{ExoMN} and $\alpha_{Fe(III)ExoMN}$ are the usual Ringbom coefficients[42] for ExoMN and the Fe(III)−ExoMN complex, respectively. The pFe for ExoMN was calculated to be 31.1, which is greater than the values calculated for most natural siderophores (Table 3), and is significantly higher than that of transferrin, 23.6.[44] This shows a remarkable affinity of ExoMN for Fe_{aq}^{3+}.

Electrochemistry and Fe(II) Chelation. Reversible electrochemistry is illustrated by the cyclic voltammogram for Fe(III)−ExoMN (Figure 4) corresponding to an Fe(III)/Fe(II) couple with a half wave potential ($E_{1/2}$) of −595 mV versus NHE at pH = 10.8 (Table 3). The negative reduction potential for the Fe(III)/Fe(II) couple indicates that ExoMN has a much greater chelation selectivity for Fe(III) over Fe(II). This selectivity is directly related to the stability constant of Fe(III)- and Fe(II)-complexes of ligand ExoMN and is described by eq 15, where β_{110}^{III} and β_{110}^{II} represent the overall stability constants

$$E_{aquo} - E_{complex}^{\circ} = 59.15 \log(\beta_{110}^{III}/\beta_{110}^{II}) \quad (15)$$

for the Fe(III) and Fe(II) oxidation states, respectively. The $Fe(II)ExoMN^{-}$ stability constant for ExoMN was calculated using eq 15 and is listed in Table 3.

The pH dependence of the cyclic voltammogram shows a gradual positive shift in the reduction potential for the Fe(III)/Fe(II) couple as the pH is lowered. The cyclic voltammogram remains reversible until pH = 10.4. As the pH is lowered below pH = 10.4, the voltammogram becomes quasi-reversible until pH = 7. The observed $E_{1/2}$ is strongly pH dependent (Figure 4, inset) and is attributed to protonation of the Fe(II)− and Fe(III)−ExoMN complexes over the experimental pH range. The pH dependence of the reduction potential profile in Figure 4, inset, corresponds to three distinct single protonation reactions, as described below.

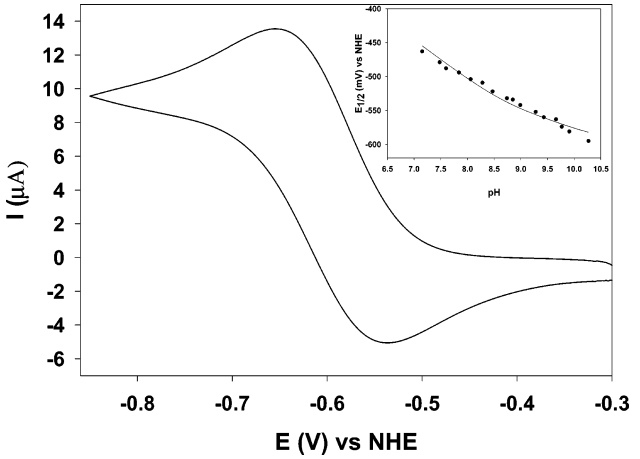

Figure 4. Cyclic voltammogram of Fe(III)−exochelin MN complex. Conditions: [Fe] = 5×10^{-3} M, [ExoMN] = 3.5×10^{-2} M, pH = 10.8. HDME working electrode, scan rate = 20 mV/s, T = 298 K, and I = 0.10 M ($NaClO_4$). $E_{1/2}$ = −595 mV with a peak separation of 112 mV. Inset: Fe(III)−exochelin MN reduction potential ($E_{1/2}$) as a function of pH. Conditions: [Fe] = 5×10^{-3} M, [ExoMN] = 3.5×10^{-2} M. HDME working electrode, scan rate = 20 mV/s, T = 298 K, and μ = 0.10 M ($NaClO_4$). The solid line represents a fit of eq 23 to the data where the following two parameters were fixed ($E_{1/2}$ = −595 mV and, as defined in eqs 21 and 22 and Scheme 2, log $K_{Fe(III)HExoMN(H_2)} = 10^{9.61}$), and log $K_{Fe(II)HExoMN(H_2)}$ and log $K_{Fe(II)H_2ExoMN(H_2)}$ (defined in eqs 17−20) were allowed to float and were determined by nonlinear least-squares analysis to be $10^{10.3}$ and $10^{8.9}$, respectively.

Over the experimental pH range, $Fe(III)ExoMN(H_2)^{2+}$, $Fe(III)ExoMN(H)^{+}$, and Fe(III)ExoMN are present in the solution with $Fe(III)ExoMN(H_2)^{2+}$ being the most predominant form of Fe(III)−ExoMN (Figure 3). The observed positive shift in the $E_{1/2}$ with decreasing pH can be modeled using first coordination sphere protonation of the Fe(II)- and Fe(III)-complexes, and assuming that the second coordination sphere protonation does not significantly influence the $E_{1/2}$. The model is based on three protonation equilibria, two corresponding to the protonation reactions of the reduced Fe(II)−ExoMN complex and one corresponding to the protonation of the Fe(III)−ExoMN complex.

The $Fe(III)ExoMN(H_2)^{2+}$ complex undergoes reduction as described by eq 16 to give $Fe(II)ExoMN(H_2)^{+}$. The reduction is then followed by two successive protonations as described by eqs 17−20. The first of the two protonation steps corresponds to the protonation of the amine nitrogen coordinated to Fe(II), resulting in an isomer flip in the first coordination shell of iron where the imidazole nitrogen replaces the amine nitrogen.

$$Fe(III)ExoMN(H_2)^{2+} \overset{+e^-}{\rightleftharpoons} Fe(II)ExoMN(H_2)^{+} \quad (16)$$

$$Fe(II)ExoMN(H_2)^{+} + H^{+} \overset{K_{Fe(II)HExoMN(H_2)}}{\rightleftharpoons} Fe(II)HExoMN(H_2)^{2+} \quad (17)$$

(37) Schwarzenbach, G.; Schwarzenbach, K. *Helv. Chim. Acta* **1963**, *46*, 1390−1400.
(38) Wong, G. B.; Kappel, M. J.; Raymond, K. N.; Matzanke, B.; Winkelmann, G. *J. Am. Chem. Soc.* **1983**, *105*, 810−815.
(39) Anderegg, G.; L'Eplattenier, F.; Schwarzenbach, G. *Helv. Chim. Acta* **1963**, *46*, 1409−1422.
(40) Loomis, L. D.; Raymond, K. N. *Inorg. Chem.* **1991**, *30*, 906−911.
(41) Albrecht-Gary, A.-M.; Blanc, S.; Rochel, N.; Ocaktan, A. Z.; Abdallah, M. A. *Inorg. Chem.* **1994**, *33*, 6391−6402.
(42) Ringbom, A. *Complexation in Analytical Chemistry: A Guide for the Critical Selection of Analytical Methods Based on Complexation Reactions*; Interscience Publishers: New York, 1963.
(43) Raymond, K. N.; Müller, G.; Matzanke, B. F. In *Topics in Current Chemistry*; Boschke, F. L., Ed.; Springer-Verlag: Berlin, Heidelberg, 1984; Vol. 123, pp 49−102.
(44) Harris, W. R.; Carrano, C. J.; Cooper, S. R.; Sofen, S. R.; Avdeef, A.; McArdle, J. V.; Raymond, K. N. *J. Am. Chem. Soc.* **1979**, *101*, 6097−6104.

$$K_{\mathrm{Fe(II)HExoMN(H_2)}} = \frac{[\mathrm{Fe(II)HExoMN(H_2)^{2+}}]}{[\mathrm{Fe(II)ExoMN(H_2)^{+}}][\mathrm{H^+}]} \quad (18)$$

$$\mathrm{Fe(II)HExoMN(H_2)^{2+}} + \mathrm{H^+} \overset{K_{\mathrm{Fe(II)H_2ExoMN(H_2)}}}{\rightleftharpoons} \mathrm{Fe(II)H_2ExoMN(H_2)(H_2O)^{3+}} \quad (19)$$

$$K_{\mathrm{Fe(II)H_2ExoMN(H_2)}} = \frac{[\mathrm{Fe(II)H_2ExoMN(H_2)(H_2O)^{3+}}]}{[\mathrm{Fe(II)HExoMN(H_2)^{2+}}][\mathrm{H^+}]} \quad (20)$$

The predominant form of the Fe(III)−ExoMN complex, $Fe(III)ExoMN(H_2)^{2+}$, over the experimental pH range can be protonated as the pH is lowered, as described by eqs 21 and 22.[21]

$$\mathrm{Fe(III)ExoMN(H_2)^{2+}} + \mathrm{H^+} \overset{K_{\mathrm{Fe(III)HExoMN(H_2)}}}{\rightleftharpoons} \mathrm{Fe(III)HExoMN(H_2)^{3+}} \quad (21)$$

$$\mathrm{K_{Fe(III)HExoMN(H_2)}} = \frac{[\mathrm{Fe(III)HExoMN(H_2)^{3+}}]}{[\mathrm{Fe(III)ExoMN(H_2)^{2+}}][\mathrm{H^+}]} \quad (22)$$

This protonation corresponds to the protonation of amine nitrogen coordinated to Fe(III) and results in a proton-driven coordination isomerization of the Fe(III)-complex. For such a system, with three distinct protonation steps, the observed formal reduction potential should vary as

$$E_f = E_{1/2} + 59.15 \log(1 + K_{\mathrm{Fe(II)HExoMN(H_2)}}[\mathrm{H^+}] + K_{\mathrm{Fe(II)HExoMN(H_2)}}K_{\mathrm{Fe(II)H_2ExoMN(H_2)}}[\mathrm{H^+}]^2) - 59.15 \log(1 + K_{\mathrm{Fe(III)HExoMN(H_2)}}[\mathrm{H^+}]) \quad (23)$$

where $E_{1/2}$ is the redox potential of $Fe(III)ExoMN(H_2)^{2+}$, $K_{\mathrm{Fe(II)HExoMN(H_2)}}$ and $K_{\mathrm{Fe(II)H_2ExoMN(H_2)}}$ are the stepwise protonation constants of the Fe(II)-complex, and $K_{\mathrm{Fe(III)HExoMN(H_2)}}$ is the protonation constant of the Fe(III)-complex. A nonlinear least-squares refinement of the data (Figure 4, inset) using eq 23 with a fixed $K_{\mathrm{Fe(III)HExoMN(H_2)}}$ value of $10^{9.61}$ obtained from the potentiometric titration gave two Fe(II)-complex protonation constants which are listed in Table 2.

Discussion

The high overall stability of the Fe(III)ExoMN complex, as compared to most natural siderophore systems (Table 3), and the presence of a rare β-hydroxyhistidine moiety as one of the Fe(III) chelating groups, make ExoMN an unusual siderophore. The proton-dependent equilibrium studies indicate protonation at both the first and the second coordination shell of Fe(III)-ExoMN. The protonation at the first coordination shell first involves a coordination isomerization and then a dechelation process. In the case of the Fe(III)−ExoMN complex, the initial protonation at the first coordination shell of Fe(III) results in a shift in the Fe(III) coordination mode in which an amine donor is substituted by an imidazole group on the β-hydroxyhistidine moiety. This protonation controls the coordination isomer flip in Fe−ExoMN. Such a proton-dependent interconversion of two different coordination isomers is rare in siderophore chelates.[45−47] This is the first instance with direct spectrophotometric evidence of a dynamic equilibrium involving coordination isomerization in a siderophore complex. The subsequent protonations in the first coordination shell of Fe(III) result in a stepwise dechelation process beginning with the protonation of the hydroxy group on the β-hydroxyhistidine moiety, followed by protonation of the imidazole group. This is the first ever determination of the protonation constants for such a moiety. The subsequent protonations result in dechelation of the hydroxamate moieties. Only one of the protonation constants for the hydroxamate groups could be calculated, and it is in very good agreement with those calculated for other siderophore systems.[39,48] The second coordination shell protonation occurs at two free amine groups, a primary and a secondary amine, and does not involve a dechelation process. These second coordination shell protonation constants are very similar to those seen for the second coordination shell protonation of a free amine group in other natural siderophores[39,48] and are also in very good agreement with the protonation constants calculated for ExoMN in the absence of Fe(III).

The stepwise protonations, coordination isomerization, and dechelation are illustrated in Scheme 2 along with the protonation constants. The protonation constants are also separately listed in Table 2. The pK_a values and $K_{\mathrm{Fe(III)H_nExoMN(H_n)}}$ protonation constants are related as they describe a proton dissociation and a protonation reaction, respectively, in opposite directions, and a representative relationship is illustrated below.

$$\mathrm{Fe(III)HExoMN(H_2)} \underset{K_{\mathrm{Fe(III)HExoMN(H_2)}}}{\overset{K_5}{\rightleftharpoons}} \mathrm{Fe(III)ExoMN(H_2)} + \mathrm{H^+} \quad (24)$$

$$pK_5 = -\log K_5 = -\log(1/K_{\mathrm{Fe(III)HExoMN(H_2)}}) = \log K_{\mathrm{Fe(III)HExoMN(H_2)}} \quad (25)$$

The Fe(III)−ExoMN protonation constants along with the ExoMN protonation constants influence the species distribution at various pH values (Figure 3) and directly reflect the relative chelating ability of ExoMN at specific conditions. A more direct comparison of this effectiveness is achieved by comparing the pFe values (Table 3). The pFe of ExoMN is one of the highest among natural siderophores, despite significantly high Fe(III)−ExoMN protonation constants. This is not surprising because at pH = 7.4, where pFe is calculated, $Fe(III)HExoMN(H_2)^{3+}$ is the predominant species (Figure 3), where all six coordination sites in Fe(III) are still occupied by ExoMN as a result of the proton-dependent isomer flip. The high pFe of ExoMN indicates that it is a very effective Fe(III) chelating agent at physiological pH and, for example, is thermodynamically capable of removing Fe(III) from transferrin.

A pH-dependent electrochemical study of Fe(III)−ExoMN (Figure 4, inset) demonstrates that the $E_{1/2}$ for Fe(III)−ExoMN is very sensitive to pH changes. This sensitivity is a reflection of high Fe(II)−ExoMN protonation constants. The protonation

(45) Cohen, S. M.; Meyer, M.; Raymond, K. N. *J. Am. Chem. Soc.* **1998**, *120*, 6277−6286.
(46) Serratrice, G.; Baret, P.; Boukhalfa, H.; Gautier-Luneau, I.; Luneau, D.; Pierre, J.-L. *Inorg. Chem.* **1999**, *38*, 840−841.
(47) Dhungana, S.; Heggemann, S.; Heinisch, L.; Moellmann, U.; Boukhalfa, H.; Crumbliss, A. L. *Inorg. Chem.* **2001**, *40*, 7079−7086.
(48) Evers, A.; Hancock, R. D.; Martell, A. E.; Motekaitis, R. J. *Inorg. Chem.* **1989**, *28*, 2189−2195.

Scheme 2

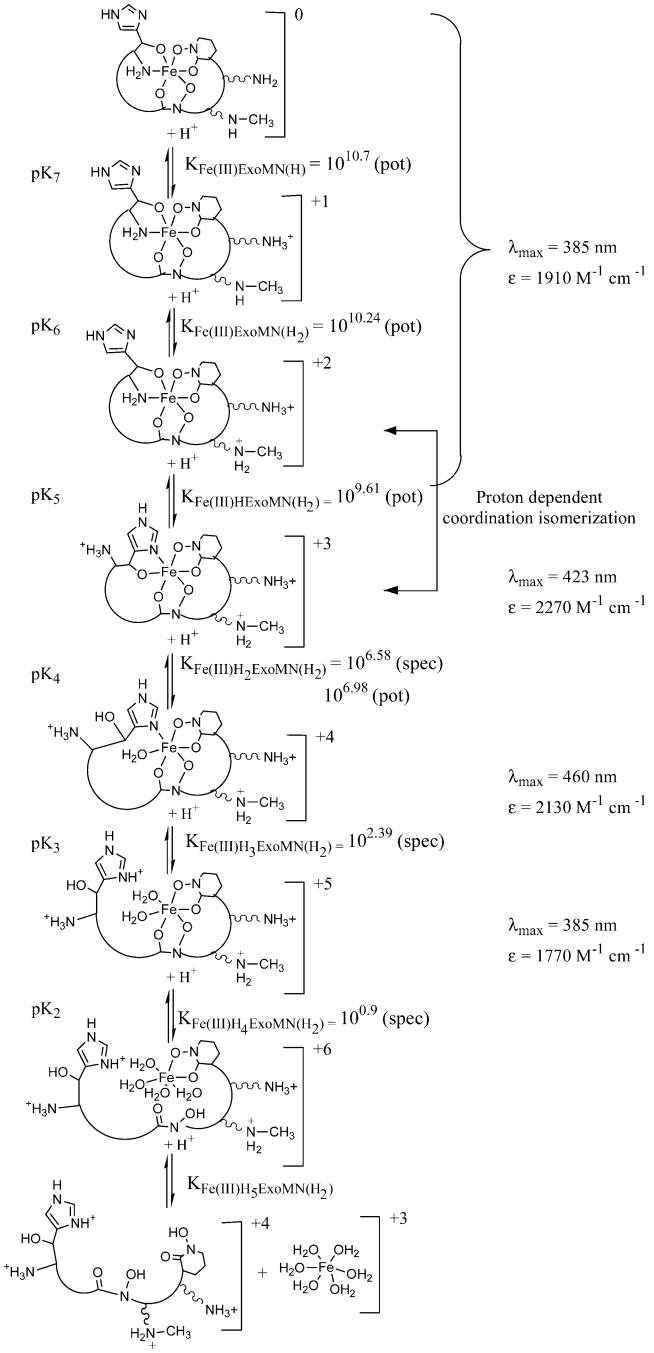

constants for the Fe(II)−ExoMN complex calculated from the pH-dependent electrochemical studies (Table 2) are significantly higher than the corresponding protonation constants for Fe(III)−ExoMN. These higher protonation constants also indicate that the proton-driven coordination isomerization for the Fe(II)−ExoMN complex occurs at a higher pH as compared to the Fe(III)−ExoMN complex. The higher protonation constants for the Fe(II)−complex as compared to the Fe(III)−complex are consistent with data for ferrioxamine B and a synthetic ferrichrome analogue and demonstrate that protonation of the Fe(II)-complex can be achieved more easily as compared to that of the Fe(III)-complex.[2,49] This observation is further support for an iron release mechanism in siderophore-mediated iron transport comprised of two complementary processes involving reduction of the Fe(III)−siderophore complex to an Fe(II)-complex and its subsequent protonation. Thus, an Fe(III/II) reduction process not only decreases the thermodynamic stability of the complex ($\beta_{110}^{III} = 10^{39.12}$; $\beta_{110}^{II} = 10^{16.7}$) and makes the complex more labile with respect to ligand exchange, but in addition makes it more susceptible to protonation.

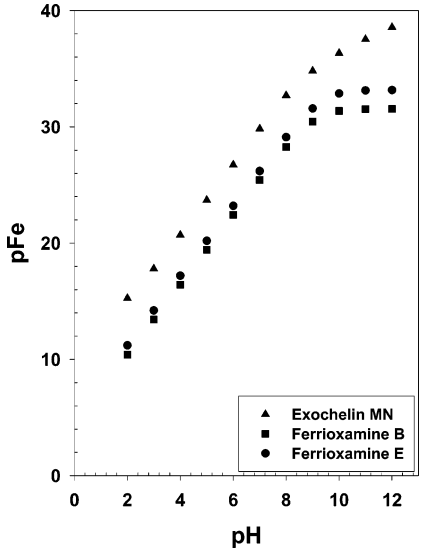

Figure 5. Calculated pFe as a function of pH. Sources of data for the calculations are as follows: exochelin MN, this work; ferrioxamine B, ref 37; ferrioxamine E, refs 56,57.

A comparative analysis of pFe as a function of pH for three different siderophores (Figure 5) shows a linear relationship between pFe and pH below a plateau region at pH ≈ 9. The pFe for ExoMN is consistently higher than that of both ferrioxamine B and ferrioxamine E in all pH ranges, suggesting that ExoMN binds Fe(III) much more effectively than both ferrioxamine B and ferrioxamine E. Such a higher effective Fe(III) binding along with its hydrophilicity, in theory, makes ExoMN a possible alternative to desferrioxamine B as a drug for chelation therapy. This application may be precluded, however, by the possible use of ExoMN bound iron by pathogens.

The exochelin MN-mediated iron uptake in *M. neoaurum* and a pathogenic *M. leprae* appears to take place by a diffusion-controlled process rather than by active transport.[22] This diffusion-controlled uptake of iron in *M. leprae*, however, cannot be sustained by other Fe(III) complexing agents such as citrate and salicylate and thus indicates that a recognition mechanism is operative. At physiological pH, Fe(III)−ExoMn is present as highly charged $Fe(III)HExoMN(H_2)^{3+}$ and $Fe(III)H_2ExoMN(H_2)^{4+}$ complexes (Figure 3) which can readily undergo a dechelation process, as $pK_4 = 6.98$, and protonation is within

(49) Dhungana, S.; Heggemann, S.; Gebhardt, P.; Moellmann, U.; Crumbliss, A. L. *Inorg. Chem.* **2003**, *42*, 42−50.
(50) Wawrousek, E. F.; McArdle, J. V. *J. Inorg. Biochem.* **1982**, *17*, 169−183.
(51) Bickel, H.; Hall, G. E.; Keller-Schierlein, W.; Prelog, V.; Vischer, E.; Wettstein, A. *Helv. Chim. Acta* **1960**, *43*, 2129−38.
(52) Cooper, S. R.; McArdle, J. V.; Raymond, K. N. *Proc. Natl. Acad. Sci. U.S.A.* **1978**, *75*, 3551−3554.
(53) Spasojevic, I.; Armstrong, S. K.; Brickman, T. J.; Crumbliss, A. L. *Inorg. Chem.* **1999**, *38*, 449−454.
(54) Lee, C.-W.; Ecker, D. J.; Raymond, K. N. *J. Am. Chem. Soc.* **1985**, *107*, 6920−6923.
(55) Pecoraro, V. L.; Wong, G. B.; Kent, T. A.; Raymond, K. N. *J. Am. Chem. Soc.* **1983**, *105*, 4617−4623.
(56) Konetschny-Rapp, S.; Jung, G.; Raymond, K. N.; Meiwes, J.; Zahner, H. *J. Am. Chem. Soc.* **1992**, *114*, 2224−2230.
(57) Anderegg, G.; L'Eplattenier, F.; Schwarzenbach, G. *Helv. Chim. Acta* **1963**, *46*, 1400−1408.

the physiological pH range. The high positive charge on the Fe(III)−ExoMN complexes, in contrast to the Fe(III)-complexes of citrate and salicylate, along with some degree of molecular recognition, could very well be responsible for the ExoMN-mediated Fe(III) transport in *M. neoaurum* and *M. leprae*. The ease of protonation of the Fe(III)HExoMN$(H_2)^{3+}$ complex at a physiological pH can facilitate proton-assisted ligand exchange between ExoMN and the membrane-bound lipophilic mycobactins. Ligand exchange and iron release may be further facilitated by Fe(III)/Fe(II) reduction as the reduced Fe(II)−ExoMN complex is protonated much more readily as compared to the oxidized Fe(III)−ExoMN complex. Such pathways may result in a diffusion-controlled iron uptake facilitated by ligand exchange.

Summary and Conclusions

The Fe(III) chelation chemistry of exochelin MN was explored in aqueous solution. The thermodynamic and the spectroscopic properties of the Fe(III)-complexes are unique as the coordination of Fe(III) by ExoMN involves a rare β-hydroxyhistidine moiety. The Fe(III) binding affinity of ExoMN is greater than that reported for most siderophores. The very high pFe of ExoMN is suggestive of an effective chelating agent at physiological conditions and indicates that from a thermodynamic standpoint ExoMN can remove Fe(III) from transferrin. The proton-dependent equilibrium studies indicate that Fe−ExoMN is capable of undergoing a reversible coordination isomer flip, where amine coordination is replaced by an imidazole group. The Fe(III)−ExoMN protonation profile indicates that a significant amount of Fe(III)H_2ExoMN$(H_2)(H_2O)^{4+}$ is present with an Fe(III) coordination site occupied by a labile water molecule at physiological pH. This form of the Fe(III)−ExoMN complex can facilitate ligand exchange between ExoMN and membrane-bound lipophilic mycobactins. A comparative analysis of the Fe(III)−ExoMN and Fe(II)−ExoMN stabilities and protonation constants illustrates that one of the iron release mechanisms is likely the reduction of the Fe(III)−siderophore followed by protonation of the Fe(II)−siderophore and subsequent release of iron. Over the physiological pH range, both ExoMN and its Fe(III)-complex are highly hydrophilic as they have a high net positive charge. This is consistent with exochelin MN's role as an extracellular siderophore.

Acknowledgment. We thank the National Science Foundation (A.L.C.; CHE-0079066) and the National Institutes of Health (M.J.M.) for financial support.

JA029578U